Published by
NIGERIAN SOCIETY OF PHYSICAL SCIENCES
Available online @ https://journal.nsps.org.ng/index.php/jnsps

J. Nig. Soc. Phys. Sci. 3 (2021) 360–384

Journal of the Nigerian Society of Physical Sciences

Computational studies on Emodin ($C_{15}H_{10}O_5$) from Methanol extract of *Pteridium acquilinum* leaves

M. E. Khan[a], E. E. Etim[b,], V. J. Anyam[c], A. Abel[d], I. G. Osigbemhe[e], C. T Agber[f]

[a]*Department of Chemistry, Federal University Lokoja, Kogi State, Nigeria*
[b]*Department of Chemical Science, Federal University Wukari Taraba State Nigeria*
[c]*Department of Chemistry University of Agriculture Makurdi, Benue State Nigeria*
[d]*Department of Pure and Applied Chemistry, Adamawa State University, Mubi, Adamawa State Nigeria*
[e]*Department of Industrial Chemistry, Federal University Lokoja, Kogi State, Nigeria*
[f]*Department of Chemistry, Benue State University, Makurdi, Benue State, Nigeria*

Abstract

This research isolated, characterized, and studied the computational and frequency calculations of emodin, extracted from the leaf extract of *Pteridium acquilinum* using methanol. Vacuum liquid and tin layer Chromatographic techniques were used for the purification of the molecule. The (VLC purified), fraction was analyzed by Nuclear magnetic resonance (NMR) and the chemical structure of the compound isolated (anthraquinone), was confirmed by ^{1}H & ^{13}C-NMR analyses as emodin **($C_{15}H_{10}O_5$)**

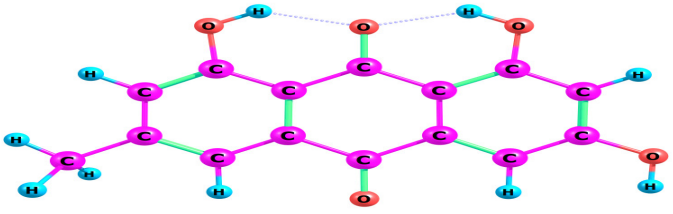

Computational and frequency studies were done on the isolated molecule. Optimized geometry, IR frequencies, Bond distances (R) and angles (A), Dipole moments and other parameters have been computationally determined for the isolated molecule from quantum chemical calculations using the GAUSSIAN 09 retinue programs. Experimentally determined and computationally measured IR frequencies agreed perfectly with each other. Computational studies have been used to predict unobserved chemical phenomena like design of new drugs and materials such as the positions of constituent atoms in relationship to their relative and absolute energies, electronic charge densities, dipoles, higher multiple moments, vibrational frequencies, relativity or other spectroscopic quantities and cross sections for collision with other molecules. This is the first time this anthraquinone, [emodin], with most of the parameters examined is reported from *P. aquilinum*.

DOI:10.46481/jnsps.2021.301

Keywords: *Pteridium aquiilinum*, Isolated & characterized, Chromatography, Emodin, Optimized geometry, Computational and frequency studies.

Article History :
Received: 14 July 2021
Received in revised form: 14 October 2021
Accepted for publication: 01 November 2021
Published: 29 November 2021

Communicated by: B. J. Falaye

1. Introduction

The phenomenon of screening plants for the presence of phyto-molecules of medicinal importance is common place. Natural products have pharmaceutical / pharmacological activity that are useful in treating diseases and are the starting points for drugs discovery from which synthetic drug analogues can be prepared with improved efficacy, potency, safety and purity [1], when isolated, synthetic strategies and tactics are used by organic Chemists providing challenging mechanisms that permit the biologically active product to the target site. A review reported that 577 plant species have been used traditionally due to the secondary metabolites in them, [2 & 3]. Africa is blessed with its natural pharmacy of variety of plants. Chemists take the pain to analyse these plants‘ secondary metabolites for the benefit of mankind as they are precursors for modern drugs, [4]. Based on this concept and theory, the optimal geometry of the eagle fern was calculated. *Pteridium aquilinum*, brake or common bracken, also known as ”eagle fern,” is a species of fern occurring in temperate and subtropical regions in both hemispheres. The extreme lightness of its spores has led to its global distribution, [5]. The large, roughly triangular fronts of the fern are herb-like rhizomes produced singly, arising upwards from an underground, and grow to 1–3 m (3–10 ft) tall; the main stem, or stipe is up to 1 cm (0.4 in) diameter at the base. It is an adaptable plant, which readily colonies disturbed areas. It is a vascular plant that reproduces via spores and has neither seeds nor flowers. It differs from moss by being vascular and it‘s of the class *Polypodiopsidae*. They are the best house purifying plants with their evergreen leaves that help rid the home of harmful toxins and improve humanity by helping to restore moisture to air naturally and also combat winter dryness by raising indoor humidity. They are used as cooked vegetable in Baffousam (Cameroon) and consume with *Vernonia amygdalina, Delile* and *triumfetta rhomboidae*. When soaked in wood ash for 24 – 36 hours, free tannic acids are removed and the crosiers consumed and sold as “warabi” or “zenmai in Japan. Rhizomes are consumed in France, Madagascar, and the Canary Island and also used as starch and confections. Leaves are used as straw and bedding for cattle, also to filter oil and palm wine. In Cote d‘Ivoire, powdered crosiers are applied to old wounds and also as enema to overcome sterility in women. The rhizomes are mixed with *Zingiber officinal* in juice form and taken as aphrodisiac and with others to calm mental disability. In China, water soaked leaves are used as pesticides. The ash used in Europe for glass and soap production, [6].

Studies carried on *Pteridium acquilinumin* included, potential and historical uses for braken (L) Kuhn, in organic agriculture where the braken were considered a serious weed species, due to toxic constituents and negativity on agriculture and conservation, [7]. The resistance of *P. acquilinum* (L)Kuhn, to insect attack by *Trichoplusia n*i (Hubn) where dried braken leaf meals and extracts of the leaf was incorporated into an artificial diet for *trichoplusia ni* larvae and studied, [8]. Isolation and characterization of the bio assay active molecule(s) from the extract of the leaves of *Pteridium acquilinum* using the aqueous and methanolic leaf extracts was carefully examined and the extracts used in boosting some female rats hormones, [2]. The plant has many chemical compounds such as emodin, quercetin, shikimic acid, prunasin, ptaquiloside and a ‘bleeding factor’ of other known and unknown structures [9]

Almost every health challenge in the world has a solution in natural products. Thus, the discovery of pharmaceutical drugs remains one of the preeminent tasks in biomedical and related research areas. Advances in science and technology coupled with the development of quantum chemistry, new computational models and software including user-friendly interfaces have reduced the barriers to the application of computational tools in the discovery and structure elucidation of natural products. Consequently, the use of computational chemistry software as a tool to discover and determine the structure of natural products has become more common in recent years. There are several reports of recent studies where computational chemistry is applied to facilitate the discovery and structure elucidation of various natural products with the view to giving insights about the isolated compounds, [10, 11, 12, 13 & 14].

Computational studies are based on quantum mechanics and basic physical constants, with involvement of approximations, but tractable; thus, help find entirely new chemical objects. They are used to find a starting point for a laboratory synthesis or to assist in understanding experimental data such as position and source of spectroscopic peaks and to predict the possibility of entirely unknown molecules or to explore reaction mechanisms not readily studied via experiments. This work is thus, designed to carry out the characterization and identification of bioactive compounds from *P. aquilinum* leaf extracts and the quantum chemical calculations are employed to further scrutinised and give a better insight about the isolated molecule for the enhancement of human life.

2. Materials and Methods

2.1. Sample Collection and Authentication

Leaves of *P. acquilinum* that were still green but matured, were collected in and around Michika L. G. A, Adamawa State on 28th July 2014. Authentication of the plant species was by [15], in the State Ministry of Forestry, Mubi North LGA, Adamawa State and a specimen of the plant was kept in their Herbarium. The Forestry Herbarium Index number (FHI) is 1030.

2.2. Preparation of the plant Sample

Leaves of the plant were properly washed with running tap water to avoid dust and other unwanted materials that most have accumulated on the leaves from their natural habitat. Then, dust free leaves were kept to dry under shade in the Chemistry laboratory of Adamawa State University Mubi. These dried leaves were pulverized by using mortar and pestle. Finally, fine powder was obtained from the pulverized leaves by sieving through the kitchen strainer and used for extraction.

Email address: emmaetim@gmail.com (E. E. Etim)

2.3. Successive Extractions using Microwave Assisted Extraction (MAE)

250g of the powdered sample was poured into a glass (2.5 L) and 500cm^3 of normal-hexane was added to it. The bottle was then put into the microwave set at defrost every 3 minutes and removed and cooled. This was Repeated 10 times. After filtration, the residues were further extracted similarly using ethyl acetate followed by methanol, [16], and the yields thus: N-hexane, 10g, ethyl acetate, 15g and methanol, 28g respectively.

2.4. Vacuum Liquid Chromatography (VLC)

15g of the methanol extract was dissolved and mixed with celite and left to dry. The dried mixture was then loaded on the VLC that had already been packed with silica gel. It was then rinsed 20 times with 20 cm^3 each of n-hexane and ethyl acetate. Ethyl acetate - methanol gradient was used to elute the column and 60 fractions collected.

2.5. Thin Layer Chromatography

TLC was carried out on all the fractions using a solvent gradient system of 9:1 v/v chloroform in methanol. Fractions 12-19 were combined and allowed to dry. The dried sample was then dissolved in methanol but yellow crystals were left undissolved. This was carefully washed. A yellow component was thus purified, spotted on the TLC plate and was labelled (F1), [17]

2.6. Sephadex column

Dissolved components of fractions 12-19, were put on a column loaded with sephadex and eluted with solvent gradient system of 1:3:3 v/v/v methanol, chloroform and ethyl acetate. Seven (7) fractions of 2 cm^3 each were collected and spotted on the TLC plate labelled (a) and (b)

2.7. Analysis with Nuclear Magnetic Resonance (NMR) Machine

Fraction (a), RF: 0.65, of the VLC, (with a yellow colour) that was purified with the Sephadex column was sent for NMR analyses. The NMR spectra were run at SIPBS, University, Strathclyde, Glasgow, United Kingdom on JEOL-LA-400 MHz FT-NMR spectrophotometer [2].

2.8. Quantum Chemical Calculations

Current advances in theoretical and computational thermodynamics have made it easier to study systems, molecular interactions, reactions and predict parameters which would have been experimentally impossible or very difficult to study. The GAUSSIAN 09 retinue of programs was used for all the quantum chemical calculations reported here. The molecule was optimized at the M06-2X level of theory with the 6 - 31g (d,p) 6 - 31+G* basis set. The M06-2X functional is a high-nonlocal functionality with double amount of nonlocal exchange (2X). The optimized structure was stable with real frequencies as shown from the frequency calculations [18, 19, 20, 22-26].

3. Results and Discussion

Detailed computational and frequency studies of the molecule was done and all thermodynamic parameters investigated. This could help to properly identify and justly place the molecule in its chemical context and use it adequately in bioactivity studies and for some bioassays in researches. These investigations and detail analyses were carried out with the aid of Chromatography (VLC, TLC and Sephadex) and other available spectroscopic techniques like Nuclear magnetic resonance (NMR) (^{1}H & ^{13}C-NMR). The computational and frequency studies were carried out using GAUSSIAN 09 retinue programs thus; Levels of theory set: HF/6-311G, Charge = 0, Multiplicity = 1, Stoichiometry $C_{15}H_{10}O_5$, Framework group $C_1[X(C_{15}H_{10}O_5)]$, Deg. of freedom: 84, Full point group : C_1, Largest Abelian subgroup :C_1. Largest concise Abelian subgroup: C_1, Van-Der-Waal spheres, IR & Raman spectra, Bond distances (R) and angles (A), Dipole moments; field –independent basis (Debye), Rotational constants, HOMO-LUMO structures, Molecular Orbital levels and the Band gaps of: 0.33925 were investigated to bring the structural definition of the molecule, as 'emodin'

Qualitative TLC, results of *P. aquilinum* leaf extract (**Table 1**), performed on the methanol crude extracts are presented and discussed. The two spots detected on the TLC plate of the sephadex column fraction; yellow colour, implied that there are two different components in the extract. Retention factor (Rf) = distance travelled by the solution/ distance travelled by the solvent front; Rf (Fa) = 2.2/3.7 = 0.59 and Rf (Fb) = 2.5/3.7 = 0.68.

Table 1. Result of Qualitative TLC of Leaf methanol extract of *P. aquilinum*

Extract	No. of spots	R_f	Quantity
leaf	1	2.2/3.7 = 0.59	0.5mg
leaf	1	2.5/3.7=0.68	(small)

3.1. Optimized Geometry

Figure 1, portrays the optimized geometry of *P. aquilinum* isolated from the methanol extract.

Optimized geometry of *P. aquilinum,* (**Figure 1**), obtained at the M062x/6-31g (d,p) level of theory and the Van-Der-Waals sphere (**Figure 2**), are representations of emodin illustrating where a surface might reside for the molecule based on the hard cutoffs of Van-Der-Waals radii for the individual atoms making up the molecule. [12]

3.2. FTIR Spectra Data for Isolated Emodin

The FTIR spectrum displayed C-OH stretching hydroxyl groups at 3500cm^{-1}, C-H asymmetric stretching in -CH_3 at 2925 cm^{-1}, -CH_2- stretching frequency at 2900 cm^{-1}, -C=O asymmetric stretching in Carbonyl at 1750, and C-H bending in CH_3 at 1400 cm^{-1}. FTIR analysis of isolated emodin is presented in **Table 2** and it also attested to the IR spectrum of the computationally obtained levels at the M062x/6-31g (d, p) of the molecule..

Table 2. The FTIR Spectral Data and Interpretation of Isolated methanol extract

Frequency range cm -1	Vibrational mode	Remarks
3500	C –OH stretching	Hydroxyl
2925	C-H-Asymmetric stretching	-CH3
2900	C-H Stretching frequencies	-CH2-
1750	C=O Stretching	Carbonyl
1400	C-H Bending	-CH2-

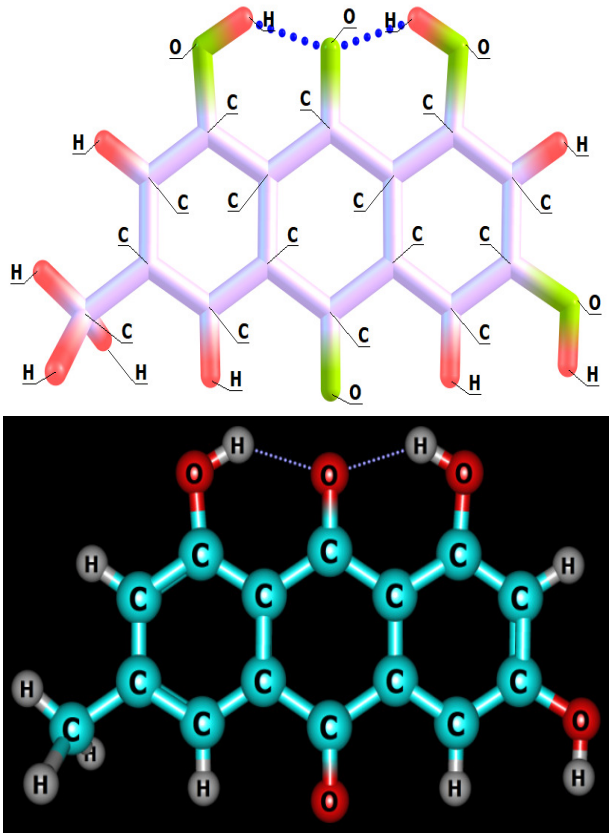

Figure 1. Models of optimized geometry of *P. aquilinum* obtained at the M06 2x /6-31g (d,p) level of theory

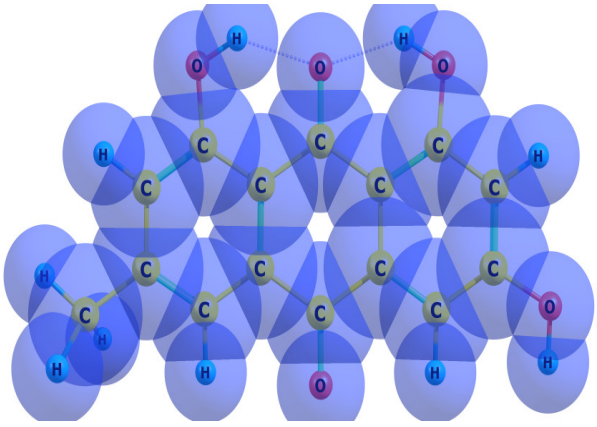

Figure 2. Van-Der-Waals sphere for *P. aquilinum* obtained at the M062x/6-31g (d, p) level of optimized geometry

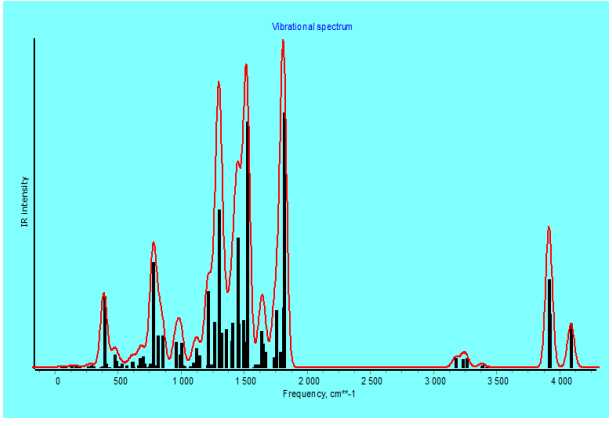

Figure 3. IR Spectrum

All the major peaks obtained experimentally are in consonance with those obtained computationally at the M062x/6-31g (d, p) level. This further validates both the experimental and computational results. The frequency from 8cm^{-1} to 3902cm^{-1} and the corresponding intensity for the IR spectrum obtained at the M062x/6-31g (d, p) level are supporting information. Regarding microwave (or rotational) spectroscopy, this molecule is active with a total dipole moment of 3.7801 Debye obtained at the M062x/6-31g (d, p) level, **Table 7.** Also, its microwave spectrum has been measured. As an asymmetric top molecule with three different moments of inertia corresponding to the three principal axes, this molecule is expected and it has three different rotational constants. At the M062x/6-31g (d,p) level, the rotational constants obtained for the molecule are 0.7462698, 0.2467690 and 0.1856618 GHz corresponding to the A, B and C rotational constants respectively, **Table 8.**

Figure 3 portrays the IR spectrum of emodin obtained at the M062x/6-31g (d, p) level of theory, ^{1}HNMR and ^{13}CNMR Spectra interpretation for methanol extract.

^{1}H NMR of the sample (**Table 3**) contains; 4 sets of aromatic peaks (7.53, 7.23, 7.12 and 6.62), two sets of phenolic peaks (12.12 and 12.06) and one set of methyl groups (2.38, attached to aromatic ring) protons.

^{13}C NMR chemical shift values (**Table 4**) revealed the presence of; 12 aromatic peaks (166.2, 164.9, 161.8, 148.7, 135.7, 133.4, 124.6, 121.0, 113.9, 109.5, 108.5 and 108.4), 2 carbonyls

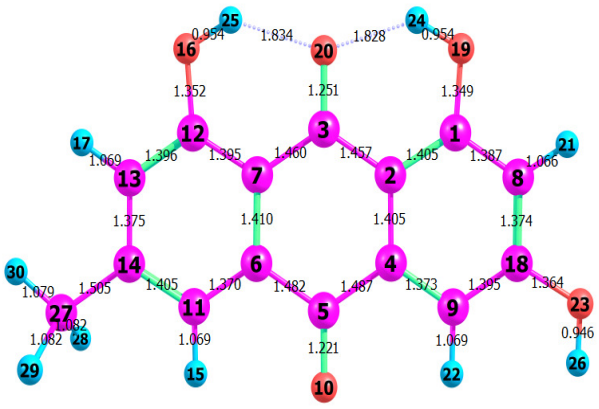

Figure 4. Bonf distances and Angles

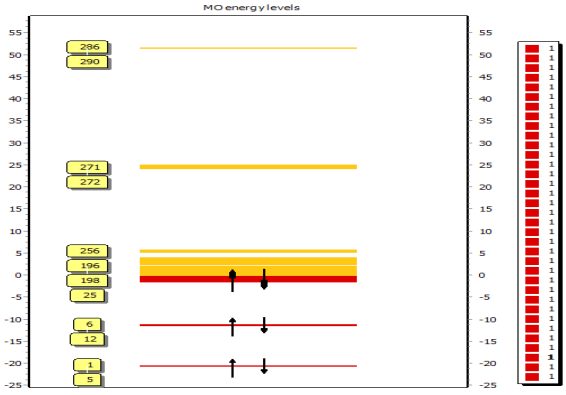

Figure 5. HOMO LUMO Diagram

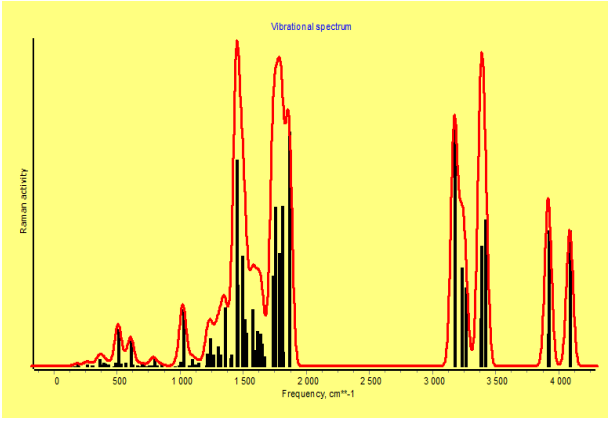

Figure 6. Raman Spectra

(190.7 and 182.2) and methyl (22.0, benzylic) carbons. This inferred that there were two aromatic nuclei that were joined through two carbonyl carbons. Thus, an anthraquinone. It can be suggested again that one of the aromatic nuclei of this anthraquinone contains a methyl and a hydroxyl substituent and the other contains two, hydroxyl substituents, one at position 8 and the other at 6.

Using 2D NMR spectra Correlation (COSY), Heteronuclear Single Quantum Correlation (HSQC) and Heteronuclear Multiple Bonds Correlation (HMBC), emodin was identified as (1, 6, 8-trihydroxy-3-methylemodin), which is an anthraquinone. Both 1D and 2D NMR spectra and also a comparison of the structure of the isolated molecule with literature values of same compound isolated from other plants like *Rumex japonica,* further confirmation was alluded to [21, 12 &13].

Table 3. ^{1}H NMR (400 MHz, DMSO solvent)

Position	chemical shift (δ) ppm (J in Hz)	multiplicity
1	-	-
2	7.20	1H, m
3	-	-
4	7.53 (1.57)	1H, d
5	6.62 (2.40)	1H, d
6	-	-
7	7.14 (2.39)	1H, d
8	-	
9	-	-
10	-	-
11	-	-
12	-	-
13	-	-
14	-	-
3-CH3	2.43	3H, s
1-OH	2.06	1H, s
8-OH	12.12	1H, s
6-OH	11.30	1H,s

Table 4. ^{13}C NMR Result (DMSO)

Position	Chemical shift (δ)	type of C
1	161.8	C
2	124.6	CH
3	148.7	C
4	121.0	CH
5	108.4	CH
6	166.2	C
7	109.5	CH
8	164.9	C
9	190.7	C
10	182.2	C
11	113.9	C
12	133.4	C
13	108.5	C
14	135.7	C
3-CH3	22.0	CH_3

^{1}H and ^{13}C (NMR) of the spectra were recorded on NMR machine: JEOL-LA-400 MHz FT-NMR spectrophotometer, at SIPBS, University, Strathclyde, Glasgow, United Kingdom, using deuterated solvents as indicated by **Tables 3 and 4.**

3.3. Bond Distances and Bond Angles

Figure 4 is the optimized geometry of Emodin showing the atomic numbers. These numbers help in determining the

distance between two atoms (say atoms 3 and 5) and the angles between atoms. **Table 6** of the supporting information contains the complete bonds distances (in Angstrom) and bond angles (in degrees), of Emodin isolated from the methanol extract.

3.4. Homo- Lumo Diagram

Here electron flow, shows whether there is constructive overlap / bonding interaction, or not, between the orbital of the HOMO and those of the LUMO. It also indicates that the orbitals are either occupied or unoccupied, **Table 9** and **Figure 5**. When the overlap is favourable, electron movement is symmetry allowed. The computational calculations have validated the theory of this interaction.

3.5. Raman Spectra

This provided good information about the structure of emodin. In this write up, the phase and the polymorphy, crystalline and molecular interactions of the atoms were computed and they tallied with the theory. (See **Figure 6** and **Table 10**).

Table 5: IR Values (Frequencies: CM^{-1} and their intensities)

Frequency, cm^{-1}	IR Intensity
40.5889	1.7505
58.1541	0.1401
72.4885	0.1147
123.9918	3.1669
152.1424	2.1859
180.5744	0.4699
185.0588	1.6663
255.505	3.307
256.5763	0.0736
277.7802	4.6633
294.7906	0.2492
297.6356	2.5751
351.015	0.4827
366.8926	1.6488
382.5217	190.7134
400.1286	9.5094
420.2978	0.9179
464.6792	34.443
477.8178	16.8814
505.9458	1.3444
520.2946	9.4524
557.7997	4.895
605.0876	14.3639
606.812	13.8679
613.2264	0.8377
652.8296	4.129
665.3268	23.4006
686.8013	28.6752
701.3117	10.2161
717.2705	0.6281
737.3912	2.1851
744.8034	9.2651
772.1549	283.7709
786.5867	5.1204
806.2587	84.9909
844.6811	86.8029
845.4904	24.5256
949.8981	67.5742

Continued on next page

Table 5 – *Continued from previous page*

Frequency, cm^{-1}	IR Intensity
980.7929	33.8411
991.5636	66.5423
1008.3375	5.9754
1019.5568	2.2067
1063.7093	1.3686
1087.4272	13.171
1110.4729	52.0946
1138.1731	32.1339
1196.3708	5.8936
1205.8194	206.5051
1230.0187	7.0492
1253.0616	123.2033
1291.437	224.8896
1294.8107	424.9948
1311.5505	92.2745
1348.5262	102.8252
1393.5713	71.2756
1400.046	119.8228
1440.4723	349.6365
1449.158	118.6796
1486.7681	127.3453
1504.6975	67.6164
1515.7165	664.1199
1563.6894	1.0644
1577.6142	7.1853
1599.795	7.4221
1627.5681	97.4458
1640.3534	10.8432
1642.8372	63.6547
1660.0202	41.9661
1725.1233	26.9024
1743.1457	155.4465
1779.4404	42.6281
1800.8258	161.4526
1805.9447	688.232
1858.3537	0.0332
3168.3115	25.498
3223.758	22.4323
3253.8947	25.0516
3375.7378	3.6376
3377.4741	1.6247
3378.858	5.0178
3411.1628	0.2215
3907.6476	236.8743
3914.4907	145.2159
4084.1357	117.2641

Structural illustrations of Bond Distance and Bond Angles

Table 6: Numerical values of bond distances and Angles

R(1-2)	1.405

Continued on next page

Table 6 – *Continued from previous page*

R(1-8)	1.387
R(1-19)	1.349
R(2-3)	1.457
R(2-4)	1.405
R(3-7)	1.460
R(3-20)	1.251
R(4-5)	1.487
R(4-9)	1.373
R(5-6)	1.482
R(5-10)	1.221
R(6-7)	1.410
R(6-11)	1.370
R(7-12)	1.395
R(8-18)	1.374
R(8-21)	1.066
R(9-18)	1.395
R(9-22)	1.069
R(11-14)	1.405
R(11-15)	1.069
R(12-13)	1.396
R(12-16)	1.352
R(13-14)	1.375
R(13-17)	1.069
R(14-27)	1.505
R(16-25)	0.954
R(18-23)	1.364
R(19-24)	0.954
R(23-26)	0.946
R(27-28)	1.082
R(27-29)	1.082
R(27-30)	1.079
R(20-24)	1.828
R(20-25)	1.834
A(2-1-8)	120.5
A(2-1-19)	123.3
A(1-2-3)	121.1
A(1-2-4)	118.2
A(8-1-19)	116.2
A(1-8-18)	119.8
A(1-8-21)	119.5
A(1-19-24)	113.6
A(3-2-4)	120.7
A(2-3-7)	119.6
A(2-3-20)	120.2
A(2-4-5)	120.3
A(2-4-9)	121.4
A(7-3-20)	120.1
A(3-7-6)	120.8
A(3-7-12)	121.1
A(3-20-24)	105.4
A(3-20-25)	105.5
A(5-4-9)	118.3
A(4-5-6)	118.4

Continued on next page

Table 6 – *Continued from previous page*

A(4-5-10)	120.4
A(4-9-18)	119.1
A(4-9-22)	119.4
A(6-5-10)	121.2
A(5-6-7)	120.1
A(5-6-11)	118.8
A(7-6-11)	121.1
A(6-7-12)	118.1
A(6-11-14)	120.5
A(6-11-15)	118.9
A(7-12-13)	120.2
A(7-12-16)	123.9
A(18-8-21)	120.7
A(8-18-9)	121.1
A(8-18-23)	117.2
A(18-9-22)	121.5
A(9-18-23)	121.7
A(14-11-15)	120.6
A(11-14-13)	118.7
A(11-14-27)	119.9
A(13-12-16)	115.9
A(12-13-14)	121.3
A(12-13-17)	117.1
A(12-16-25)	113.5
A(14-13-17)	121.6
A(13-14-27)	121.4
A(14-27-28)	110.8
A(14-27-29)	110.8
A(14-27-30)	111.4
A(16-25-20)	135.9
A(18-23-26)	115.2
A(19-24-20)	136.3
A(28-27-29)	107.5
A(28-27-30)	108.1
A(29-27-30)	108.1
A(24-20-25)	149.1
W1(A)	40.6
W2(A)	58.2
W3(A)	72.5
W4(A)	124.0
W5(A)	152.1
W6(A)	180.6
W7(A)	185.1
W8(A)	255.5
W9(A)	256.6
W10(A)	277.8
W11(A)	294.8
W12(A)	297.6
W13(A)	351.0
W14(A)	366.9
W15(A)	382.5
W16(A)	400.1
W17(A)	420.3

Continued on next page

Table 6 – *Continued from previous page*

W18(A)	464.7
W19(A)	477.8
W20(A)	505.9
W21(A)	520.3
W22(A)	557.8
W23(A)	605.1
W24(A)	606.8
W25(A)	613.2
W26(A)	652.8
W27(A)	665.3
W28(A)	686.8
W29(A)	701.3
W30(A)	717.3
W31(A)	737.4
W32(A)	744.8
W33(A)	772.2
W34(A)	786.6
W35(A)	806.3
W36(A)	844.7
W37(A)	845.5
W38(A)	949.9
W39(A)	980.8
W40(A)	991.6
W41(A)	1008.3
W42(A)	1019.6
W43(A)	1063.7
W44(A)	1087.4
W45(A)	1110.5
W46(A)	1138.2
W47(A)	1196.4
W48(A)	1205.8
W49(A)	1230.0
W50(A)	1253.1
W51(A)	1291.4
W52(A)	1294.8
W53(A)	1311.6
W54(A)	1348.5
W55(A)	1393.6
W56(A)	1400.0
W57(A)	1440.5
W58(A)	1449.2
W59(A)	1486.8
W60(A)	1504.7
W61(A)	1515.7
W62(A)	1563.7
W63(A)	1577.6
W64(A)	1599.8
W65(A)	1627.6
W66(A)	1640.4
W67(A)	1642.8
W68(A)	1660.0
W69(A)	1725.1
W70(A)	1743.1

Continued on next page

Table 6 – *Continued from previous page*

W71(A)	1779.4
W72(A)	1800.8
W73(A)	1805.9
W74(A)	1858.4
W75(A)	3168.3
W76(A)	3223.8
W77(A)	3253.9
W78(A)	3375.7
W79(A)	3377.5
W80(A)	3378.9
W81(A)	3411.2
W82(A)	3907.6
W83(A)	3914.5
W84(A)	4084.1

Table 7. Dipole moment (Field –independent Basis, Debye)

X	1.9607
Y	-3.2319
Z	-0.0025
Total	3.7801

Table 8. Rot. Constants for Emodin

Rotational Constants	**GHZ**
A	0.7462698
B	0.2467690
C	0.1856618

Table 9: Numerical indicators of occupied and unoccupied molecular orbitals

1 Occupied	-20.6106 A
2 Occupied	-20.59061 A
3 Occupied	-20.58999 A
4 Occupied	-20.58463 A
5 Occupied	-20.58063 A
6 Occupied	-11.39494 A
7 Occupied	-11.38389 A
8 Occupied	-11.35976 A
9 Occupied	-11.3571 A
10 Occupied	-11.35506 A

Continued on next page

Table 9 – *Continued from previous page*

11 Occupied	-11.30275 A
12 Occupied	-11.29346 A
13 Occupied	-11.29192 A
14 Occupied	-11.28269 A
15 Occupied	-11.28221 A
16 Occupied	-11.2699 A
17 Occupied	-11.2639 A
18 Occupied	-11.26076 A
19 Occupied	-11.25788 A
20 Occupied	-11.24752 A
21 Occupied	-1.45133 A
22 Occupied	-1.443 A
23 Occupied	-1.43897 A
24 Occupied	-1.43163 A
25 Occupied	-1.4124 A
26 Occupied	-1.21648 A
27 Occupied	-1.19863 A
28 Occupied	-1.12143 A
29 Occupied	-1.07739 A
30 Occupied	-1.06499 A
31 Occupied	-1.05973 A
32 Occupied	-0.9952 A
33 Occupied	-0.9526 A
34 Occupied	-0.92195 A
35 Occupied	-0.89005 A
36 Occupied	-0.86663 A
37 Occupied	-0.83926 A

Continued on next page

Table 9 – *Continued from previous page*

38 Occupied	-0.79888 A
39 Occupied	-0.77404 A
40 Occupied	-0.76007 A
41 Occupied	-0.73987 A
42 Occupied	-0.72586 A
43 Occupied	-0.69958 A
44 Occupied	-0.69417 A
45 Occupied	-0.67067 A
46 Occupied	-0.66231 A
47 Occupied	-0.65235 A
48 Occupied	-0.64739 A
49 Occupied	-0.63103 A
50 Occupied	-0.62251 A
51 Occupied	-0.61638 A
52 Occupied	-0.60289 A
53 Occupied	-0.60155 A
54 Occupied	-0.59301 A
55 Occupied	-0.58622 A
56 Occupied	-0.58475 A
57 Occupied	-0.56457 A
58 Occupied	-0.56087 A
59 Occupied	-0.55885 A
60 Occupied	-0.54681 A
61 Occupied	-0.54236 A
62 Occupied	-0.53297 A
63 Occupied	-0.49741 A
64 Occupied	-0.48094 A

Continued on next page

Table 9 – *Continued from previous page*

65 Occupied	-0.46984 A
66 Occupied	-0.44326 A
67 Occupied	-0.37943 A
68 Occupied	-0.36226 A
69 Occupied	-0.35055 A
70 Occupied	-0.33995 A
71 Unoccupied	-0.0007 A
72 Unoccupied	0.06955 A
73 Unoccupied	0.10587 A
74 Unoccupied	0.13378 A
75 Unoccupied	0.13583 A
76 Unoccupied	0.14836 A
77 Unoccupied	0.18701 A
78 Unoccupied	0.2009 A
79 Unoccupied	0.2011 A
80 Unoccupied	0.2037 A
81 Unoccupied	0.21134 A
82 Unoccupied	0.22203 A
83 Unoccupied	0.22495 A
84 Unoccupied	0.23454 A
85 Unoccupied	0.23529 A
86 Unoccupied	0.25213 A
87 Unoccupied	0.32229 A
88 Unoccupied	0.34319 A
89 Unoccupied	0.34611 A
90 Unoccupied	0.35786 A
91 Unoccupied	0.37219 A

Continued on next page

Table 9 – *Continued from previous page*

92 Unoccupied	0.3831 A
93 Unoccupied	0.4018 A
94 Unoccupied	0.40497 A
95 Unoccupied	0.41765 A
96 Unoccupied	0.43383 A
97 Unoccupied	0.44363 A
98 Unoccupied	0.44626 A
99 Unoccupied	0.45481 A
100 Unoccupied	0.46011 A
101 Unoccupied	0.48707 A
102 Unoccupied	0.49981 A
103 Unoccupied	0.50292 A
104 Unoccupied	0.50877 A
105 Unoccupied	0.51194 A
106 Unoccupied	0.52321 A
107 Unoccupied	0.52819 A
108 Unoccupied	0.53979 A
109 Unoccupied	0.54525 A
110 Unoccupied	0.55944 A
111 Unoccupied	0.56865 A
112 Unoccupied	0.57009 A
113 Unoccupied	0.58434 A
114 Unoccupied	0.58662 A
115 Unoccupied	0.59683 A
116 Unoccupied	0.60621 A
117 Unoccupied	0.60814 A
118 Unoccupied	0.61375 A

Continued on next page

Table 9 – *Continued from previous page*

119 Unoccupied	0.61988 A
120 Unoccupied	0.62327 A
121 Unoccupied	0.62597 A
122 Unoccupied	0.62776 A
123 Unoccupied	0.63742 A
124 Unoccupied	0.65303 A
125 Unoccupied	0.65887 A
126 Unoccupied	0.66405 A
127 Unoccupied	0.67701 A
128 Unoccupied	0.68162 A
129 Unoccupied	0.68987 A
130 Unoccupied	0.69117 A
131 Unoccupied	0.69598 A
132 Unoccupied	0.7286 A
133 Unoccupied	0.73459 A
134 Unoccupied	0.75046 A
135 Unoccupied	0.75306 A
136 Unoccupied	0.76128 A
137 Unoccupied	0.77724 A
138 Unoccupied	0.77807 A
139 Unoccupied	0.77996 A
140 Unoccupied	0.80091 A
141 Unoccupied	0.80389 A
142 Unoccupied	0.81138 A
143 Unoccupied	0.81625 A
144 Unoccupied	0.82077 A
145 Unoccupied	0.83575 A

Continued on next page

Table 9 – *Continued from previous page*

146 Unoccupied	0.84813 A
147 Unoccupied	0.86274 A
148 Unoccupied	0.88017 A
149 Unoccupied	0.88642 A
150 Unoccupied	0.88885 A
151 Unoccupied	0.89606 A
152 Unoccupied	0.92417 A
153 Unoccupied	0.93098 A
154 Unoccupied	0.9795 A
155 Unoccupied	0.98929 A
156 Unoccupied	1.01128 A
157 Unoccupied	1.01814 A
158 Unoccupied	1.02265 A
159 Unoccupied	1.02918 A
160 Unoccupied	1.05372 A
161 Unoccupied	1.06017 A
162 Unoccupied	1.06199 A
163 Unoccupied	1.06346 A
164 Unoccupied	1.07991 A
165 Unoccupied	1.08652 A
166 Unoccupied	1.09138 A
167 Unoccupied	1.10578 A
168 Unoccupied	1.11793 A
169 Unoccupied	1.1187 A
170 Unoccupied	1.13433 A
171 Unoccupied	1.14179 A
172 Unoccupied	1.14713 A

Continued on next page

Table 9 – *Continued from previous page*

173 Unoccupied	1.16523 A
174 Unoccupied	1.17615 A
175 Unoccupied	1.1908 A
176 Unoccupied	1.19371 A
177 Unoccupied	1.20229 A
178 Unoccupied	1.21612 A
179 Unoccupied	1.25361 A
180 Unoccupied	1.26206 A
181 Unoccupied	1.27792 A
182 Unoccupied	1.29634 A
183 Unoccupied	1.34272 A
184 Unoccupied	1.36669 A
185 Unoccupied	1.37455 A
186 Unoccupied	1.38165 A
187 Unoccupied	1.39717 A
188 Unoccupied	1.45107 A
189 Unoccupied	1.48546 A
190 Unoccupied	1.49397 A
191 Unoccupied	1.50947 A
192 Unoccupied	1.51616 A
193 Unoccupied	1.54722 A
194 Unoccupied	1.55972 A
195 Unoccupied	1.62076 A
196 Unoccupied	1.92958 A
197 Unoccupied	1.9693 A
198 Unoccupied	1.99045 A
199 Unoccupied	2.01527 A

Continued on next page

Table 9 – *Continued from previous page*

200 Unoccupied	2.04241 A
201 Unoccupied	2.47872 A
202 Unoccupied	2.55557 A
203 Unoccupied	2.57245 A
204 Unoccupied	2.58411 A
205 Unoccupied	2.61213 A
206 Unoccupied	2.66724 A
207 Unoccupied	2.67833 A
208 Unoccupied	2.7261 A
209 Unoccupied	2.75184 A
210 Unoccupied	2.76667 A
211 Unoccupied	2.83591 A
212 Unoccupied	2.87279 A
213 Unoccupied	2.87898 A
214 Unoccupied	2.89883 A
215 Unoccupied	2.92545 A
216 Unoccupied	2.94814 A
217 Unoccupied	2.96326 A
218 Unoccupied	2.98075 A
219 Unoccupied	3.03619 A
220 Unoccupied	3.05634 A
221 Unoccupied	3.09158 A
222 Unoccupied	3.09641 A
223 Unoccupied	3.10212 A
224 Unoccupied	3.10332 A
225 Unoccupied	3.10964 A
226 Unoccupied	3.17293 A

Continued on next page

Table 9 – *Continued from previous page*

227 Unoccupied	3.23325 A
228 Unoccupied	3.248 A
229 Unoccupied	3.29189 A
230 Unoccupied	3.30673 A
231 Unoccupied	3.32245 A
232 Unoccupied	3.34172 A
233 Unoccupied	3.35642 A
234 Unoccupied	3.35848 A
235 Unoccupied	3.37538 A
236 Unoccupied	3.37812 A
237 Unoccupied	3.38723 A
238 Unoccupied	3.41087 A
239 Unoccupied	3.46033 A
240 Unoccupied	3.48637 A
241 Unoccupied	3.502 A
242 Unoccupied	3.53895 A
243 Unoccupied	3.56422 A
244 Unoccupied	3.57188 A
245 Unoccupied	3.59923 A
246 Unoccupied	3.61431 A
247 Unoccupied	3.62728 A
248 Unoccupied	3.65106 A
249 Unoccupied	3.67652 A
250 Unoccupied	3.70142 A
251 Unoccupied	3.71733 A
252 Unoccupied	3.74714 A
253 Unoccupied	3.76852 A

Continued on next page

Table 9 – *Continued from previous page*

254 Unoccupied	3.89765 A
255 Unoccupied	3.98257 A
256 Unoccupied	5.32337 A
257 Unoccupied	5.35191 A
258 Unoccupied	5.35493 A
259 Unoccupied	5.38283 A
260 Unoccupied	5.40342 A
261 Unoccupied	5.44518 A
262 Unoccupied	5.49454 A
263 Unoccupied	5.50494 A
264 Unoccupied	5.54169 A
265 Unoccupied	5.5829 A
266 Unoccupied	5.60217 A
267 Unoccupied	5.66417 A
268 Unoccupied	5.70088 A
269 Unoccupied	5.73321 A
270 Unoccupied	5.76144 A
271 Unoccupied	24.19134 A
272 Unoccupied	24.27042 A
273 Unoccupied	24.41848 A
274 Unoccupied	24.49212 A
275 Unoccupied	24.49889 A
276 Unoccupied	24.51616 A
277 Unoccupied	24.5837 A
278 Unoccupied	24.63317 A
279 Unoccupied	24.7082 A
280 Unoccupied	24.80808 A

Continued on next page

Table 9 – *Continued from previous page*

281 Unoccupied	24.81693 A
282 Unoccupied	24.83965 A
283 Unoccupied	24.88602 A
284 Unoccupied	25.00561 A
285 Unoccupied	25.02082 A
286 Unoccupied	51.55558 A
287 Unoccupied	51.58631 A
288 Unoccupied	51.59188 A
289 Unoccupied	51.59641 A
290 Unoccupied	51.60474 A

Band gap: 0.33925 A.U

Table 10: Frequencies cm^{-1} and Raman activities

Frequency, cm^{-1}	Raman Activity
40.5889	0.0308
58.1541	0.3493
72.4885	0.0255
123.9918	0.0304
152.1424	0.1427
180.5744	1.7709
185.0588	0.3809
255.505	1.9977
256.5763	1.6381
277.7802	0.0179
294.7906	0.6864
297.6356	0.4601
351.015	6.5213
366.8926	1.5406
382.5217	3.5322
400.1286	2.3964
420.2978	1.913
464.6792	0.0432
477.8178	3.0011
505.9458	35.2839
520.2946	2.4177
557.7997	3.7289
605.0876	23.6777
606.812	1.0858
613.2264	1.5184
652.8296	0.7743
665.3268	0.1479
686.8013	1.8993

Continued on next page

Table 10 – *Continued from previous page*

Frequency, cm^{-1}	Raman Activity
701.3117	0.4288
717.2705	0.0411
737.3912	0.1857
744.8034	0.5408
772.1549	0.8902
786.5867	6.7614
806.2587	0.5934
844.6811	0.2227
845.4904	1.5859
949.8981	0.3197
980.7929	0.8345
991.5636	4.1317
1008.3375	1.311
1019.5568	54.1302
1063.7093	0.7049
1087.4272	6.8712
1110.4729	1.8682
1138.1731	3.5729
1196.3708	0.5286
1205.8194	11.7034
1230.0187	26.9241
1253.0616	11.4807
1291.437	9.0978
1294.8107	18.6095
1311.5505	10.9375
1348.5262	55.9278
1393.5713	7.765
1400.046	11.0092
1440.4723	195.2705
1449.158	77.3445
1486.7681	104.1229
1504.6975	44.8716
1515.7165	31.9762
1563.6894	54.3211
1577.6142	15.8238
1599.795	32.9398
1627.5681	30.8732
1640.3534	21.3528
1642.8372	13.7481
1660.0202	9.3907
1725.1233	85.1739
1743.1457	150.3192
1779.4404	106.9382
1800.8258	151.5551
1805.9447	13.6314
1858.3537	221.7421
3168.3115	226.1542
3223.758	93.6794
3253.8947	74.8114
3375.7378	45.7586
3377.4741	59.3447
3378.858	113.9246

Continued on next page

Table 10 – *Continued from previous page*

Frequency, cm^{-1}	Raman Activity
3411.1628	138.4204
3907.6476	30.7164
3914.4907	128.1222
4084.1357	128.3823

4. Conclusion

This article is the first to have done complete computational and frequency studies on the isolated anthraquinone, "emodin" from *P. aquilinum*. Optimized geometry, IR frequencies, Bond distances (R) and angles (A), Dipole moments and other parameters have been computationally determined for the isolated molecule from quantum chemical calculations using the GAUSSIAN 09 retinue programs. Experimentally determined and computationally measured IR frequencies agreed perfectly with each other. This can be used to predict unobserved chemical phenomena like design of new drugs and materials such as the positions of constituent atoms, in relationship to their relative and absolute energies, electronic charge densities, dipoles, higher multiple moments, vibrational frequencies, relativity or other spectroscopic quantities and cross sections for collision with other molecules.

Acknowledgments

Our gratitude to Prof J. O. Igoli and SIPBS, University of Strathclyde, Glasgow, UK for their help in the analyses and the Indian Institute of Science, Bangalore for facilitating the computational calculations.

References

[1] S. Samala. & S. Veeresham "Enhanced Bioavailability of Glimepirida in the presence of Boswellic acids in streptozotocin - induced Diabetic Rat model", Natural Products Chemistry and Research **1** (2013) 166.
[2] M. E. Khan, E. T. Williams, A. Abel & I. Toma "Effects of the aqueous and methanolic leaf extracts of Pteridium aquilinum (linnaeus) on some female rats hormones", Direct Research Journal of Public Health and Environmental Technology **2** (2019). 2016 8.
[3] D. Kumar, A. Kumar & O. J. Prakash "Folliculogenesis and quickening of maturation of the follicle in the pre-ovulatory phase", Ethnopharmacol **140** (2012) 1.
[4] V. D. Bambhole & G. G. Liddewar "Antibesity effect of iris *Vericolor* and *Holoptelea integrifolia* in rats", Sachitra Aqurveda **37** (1985) 557.
[5] M. E. Alonso-Amelot & M. Avendano M "Possible association between gastric cancer and racken fern in Venezuela: An epidemiologic study", International Journal of Cancer **91** (2001) 252.
[6] W. J. Vander Burg "*Pteridium acquilinum* (L.) Kuhn [internet] Record from, PROTA4U. Grubben G.J. H & Benton, O. A. (Editors) PROTA (Plant Resources of Tropical Africa / Resouces Vegeteles de l'Afrique tropicale)" Wageningen, Neitherlands (2004). http://www.prota4u.org/search asp> Accessed June 22, 2020.
[7] E. Donely, J. Robertson & D. Robinson "Potential and historical uses for braken(L.) Kuhn in organic agriculture", Conference proceedings of the COR conference, Aberystwyth **26 -28**th (2002) 255.
[8] D. Stephen & Hendrix "The resistance of *P. acquilinum* (L.)Kuhn to insect attack by *Trichoplusia n*i (Hubn)laevae incorporation", oecologia **26** (1977) 347.
[9] T. Tzeng, H. Lu, S. Liou, C. J. chang & I. Liu "Emodin, a Natrual derivative occurring Anthraquinon Derivative, Ameliorates Dyslipidemia by Activatind AMP- Activated protein Kinase in High- Fat Diet-fed Rats", Evidence-based Complementary and Alternative Medicine **2** (2012) 1.
[10] R. R. Da Silva, P. C. Dorrestein & R. A. Quinn "Illuminating the dark matter in metabolomics", Proceedings od the National Academy of Sciences of the United States of America **112** (2015) 12549.
[11] K. Dührkop, H. Shen, M. Meusel, J. Rousu & S. Böcker "Searching molecular structure databases with tandem mass spectra using CSI: Finger ID", Proceedings od the National Academy of Sciences of the United States of America **112** (2015) 12580.
[12] O. A. Ushie, E. E. Etim, H. M. Adamu, I. Y. Chindo, C. Andrew & G. P. Khanal "Quantum Chemical Studies on Decyl Heptadecanoate (C27H54O2) Detected In Ethyl Acetae Leaf Extract of Chrysophyllum albidium", Elixir Applied Chemistry **111** (2018) 48828.
[13] O. A. Ushie, E. E. Etim, A. Onen, I. Andrew, C. Lawal & G. P. Khanal "Computational Studies of β-amyrin acetate (C32H52O2) Detected in Methanol Leaf Extract of Chrysophyllum albidium", Journal of Chemical Society of Nigeria **44** (2019) 561.
[14] S. Wolf, S. Schmidt, M. Müller-Hannemann & S. Neumann "In silico fragmentation for computer assisted identification of metabolite mass spectra", BMC Bioinformatics **11** (2010) 148.
[15] M. Admu *Traditional herbalist verse with medicinal plants of the Mubi and Michika regions of Adamawa State* (2016).
[16] J. N. Anyam, T. A. Tor-anyiin & J. O. Igoli "Studies on Dacryodes edullis II: Phytochemical and medicinal principles of boiled seed", International Journal of Current Research in Chemistry and Pharmaceutical Science **2** (2016) 32.
[17] B. J. Owolabi, O. Iyekowa, G. E. Okpara & H. C. Ndibe "Synthesis, tentative characterization and antimicrobial activities of 1-ethyl 2-methyl-4-nitroimidazole-5-thiol and its derivatives", Journal of Chemical Society of Nigeria **44** (2019) 355.
[18] E. E Etim & E. Arunan "Rotational Spectroscopy and Interstellar Molecules, Planex", News letter **5** (2015) 16.
[19] E. E. Etim, P. Gorai, A. Das, S. Charabati & E. Arunan "Systematic Theoretical Study on the Interstellar Carbon Chain Molecules", The Astrophysical Journal **832** (2016) 144.
[20] E. E. Etim, P. Gorai, A. Das & E. Runan "C5H9N Isomers: Pointers to Possible Branched Chain Inte rstellar Molecules", European Physical Journal D **71** (2017) 86.
[21] G. Shuying, B. Feng, Z. Ruonan, M. Jiankang & W. Wei "Preparative isolation of three Anthraquinones from Rumex japonicus by high speed counter-current Chromatography", Molecules **16** (2011) 1201.

[22] O. A. Ushie, E. E. Etim, H. M. Adamu, I. Y. Chindo, C. Andrew & G. P. Khanal "Quantum Chemical Studies on Decyl Heptadecanoate ($C_{27}H_{54}O_2$) Detected In Ethyl Acetae Leaf Extract of *Chrysophyllum albidium*", Elixir Applied Chemistry **111** (2017) 48828.
[23] A. I. Onen, J. Joseph, E. E. Etim & N. O. Eddy "Quantum Chemical Studies on the Inhibition Mechanism of Ficus carica, FC and Vitellaria paradoxa, VP Leaf Extracts", Journal of Advanced Chemical Sciences **3** (2017) 496.
[24] O. A. Ushie, E. E. Etim, A. I. Onen, C. Andrew, U. Lawal & G. P. Khanal "Computational Studies of β-amyrin acetate (C32H52O2) Detected in Methanol Leaf Extract of *Chrysophyllum albidium*", Journal of Chemical Society of Nigeria **44** (2019) 561.
[25] E. E. Etim, O. E. Godwin, S. A. Olagboye & M. E. Khan "Protonation in Benzyl Alcohol: Different Proton Affinities, Same Neutral Molecule", Asian Journal of Emergency Research **3** (2021) 19.
[26] . E. Etim, O. E. Godwin & S. A. Olagboye "Protonation in Heteronuclear Diatomic Molecules: Same Molecule, Different Proton Affinities", Communication in Physical Sciences **6** (2020) 835.